Effect of substitution group variation on the optical functions of -5-sulfono-7-(4-x phenyl azo)-8-hydroxy quinoline thin films

CrossMark

H.M. Zeyada*, N.A. El-Ghamaz, E.A. Gaml

Department of Physics, Faculty of Science, Damietta University, New Damietta 34517, Egypt

A B S T R A C T

-5-Sulfono-7-(4-x phenyl azo)-8-hydroxy quinoline (SAHQ)-x ligands, $x =$ NO$_2$ or CH$_3$ or Cl have poly-crystalline structure in as synthesized condition. Thermally evaporated thin films of SAHQ-x have crystal structure depending on the substitution group; SAHQ-NO$_2$ and SAHQ-Cl films have nano-crystalline structure with different degree of crystallinity and SAHQ-CH$_3$ film has amorphous structure. The changes in optical functions and therefore optical constants with substitution group variation have been calculated by using spectrophotometer measurements of the transmittance and reflectance at nearly normal incidence of light in the wavelength range 200—2500 nm. Substitution group variation influences the refractive index, dispersion parameters, optical functions and bond length of SAHQ. It has no influence on mobility, relaxation time and plasma frequency of charge carriers. The obtained optical energy gaps for SAHQ-x ligands, $x =$ NO$_2$ or CH$_3$ or Cl are 1.89, 2 and 2eV, respectively.

© 2013 Elsevier B.V. All rights reserved.

1. Introduction

Quantitative estimation of the optical properties of materials plays an important role in determining its electronic structure [1]. The evaluation of optical dispersions and other optical constants are of considerable importance for applications in integrated optical devices such as switches, filters and modulators. The complex dielectric function is an important function since we can derive other optical functions such as optical conductivity and energy loss functions from it. The complex dielectric function can be determined in many ways, using either incident photons or electrons [2–4]. Dispersion parameters can be deduced from the dispersion curve in accordance with dispersion theory. Dielectric function relates the electron transition between bands of a solid to its structure. The optical conductivity can be used to detect any further allowed interband transitions and energy loss functions provide a complete description of the response of the material to fast electrons traveling either through it or on its surface.

8-Hydroxyl-Quinoline-5 sulfonic acid and its derivatives have many technological applications such as dye sensitized solar cells [5], ion sensor devices [6] and organic light emitting diodes [7–11]. 8-Hydroxyl-Quinoline-5 sulfonic acid has donor atoms such as N, S and O that contribute greatly to their thermal and environmental

stability and enhance their electrical conductivity [12]. The presence of −N═N-group can lead to an increase in the solubility of low valent metal oxidation states due to its π acidity and presence of low-lying azo centered π* molecular orbital [13,14]. Introducing appropriate ring substituent to quinoline chromophores can influence the absorbance maximum $\lambda_{max.}$, the dipole moment μ and the shape that can be roughly quantified by the aspect ratio and the effective occupied volume [15].
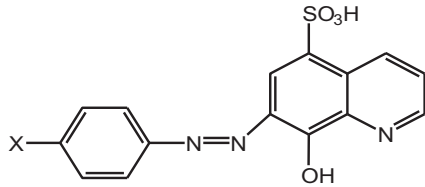
The application of -5-sulfono-7-(4-x phenyl azo)-8-hydroxy quinoline (SAHQ)-x, $x =$ NO$_2$ or CH$_3$ or Cl in device fabrication will certainly be provided as thin films. Thin films of azo compounds and their derivatives are generally prepared by chemical and physical methods, such as thermal evaporation, chemical vapor deposition, spin coating and Langmuir—Blodget deposition techniques [16—19]. The physical properties of organic compounds arises from delocalized π electrons, adsorbed species, defect sites and the presence of functional groups [20]. In this work, we report on the influence of substitution group with an effective charge +1 (NO$_2^{1+}$) and groups (Cl or CH$_3$) whose effective charge is −1 on the structure and optical functions of -5-sulfono-7-(4-x phenyl azo)-8-hydroxy quinoline (SAHQ).

2. Experimental techniques

SAHQ-x; $x =$ NO$_2$ or CH$_3$ or Cl ligands were prepared by azo coupling method using 8-hydroxy quinoline-5-sulfonic acid as a starting material for the chemical reaction and as a base material

* Corresponding author. Fax: +20 572403868.
  E-mail address: hzeyada@gmail.com (H.M. Zeyada).

Scheme 1. Molecular structure of -5-sulfono-7-(4-x phenyl azo)-8-hydroxy quinoline ligands (SAHQ-x), $x = NO_2$ or CH_3 or Cl.

for the ligands [21–23]. El-Ghamaz et al. [21] gave the detailed preparation of the materials under current investigation. Scheme 1 illustrates the molecular structure of SAHQ-x ligands. Thin films of SAHQ-X were prepared using thermal evaporation technique by a high vacuum coating unit (Edwards E306 A, England). The vacuum during the deposition process is about 10^{-5} Torr. The powder is sublimated from quartz crucible heated gradually by molybdenum boat shaped filament. A mechanical shutter was used to prevent any contamination to reach the substrates in the first stage of evaporation process and to control the thickness of the films. The deposition rate and film thickness were measured during the evaporation using a quartz crystal thickness monitor (Model TM-350 MAXTEK, Inc.USA) attached to the coating system. The determined film thickness is 223 nm. SAHQ-x thin films were deposited onto clean optically flat quartz substrates for spectrophotometric measurements and onto optically flat glass substrates for the x-ray diffraction (XRD) measurements.

The XRD measurements for the as synthesized powder and as deposited thin film of SAHQ-x ligands were carried out using **Philips** X-ray diffraction system, model **X'Pert MPD**. The X-ray diffractometer is equipped with copper target. A filtered copper $K_{\alpha 1}$ radiation with wavelength $\lambda_{k\alpha 1} = 1.540$ Å is used in the XRD measurements. The operating voltage and current for the X-ray tube were 50 kV and 40 mA, respectively. Scherer's equation [24] calculates the average crystallite size, t, as follows:

$$t = \frac{0.95\lambda}{\gamma \cos\theta}, \tag{1}$$

where γ is the width measured in radians of the half-maximum peak intensity, λ is the X-ray wavelength and θ is the Bragg's angle. The dislocation density, δ, is the number of dislocation lines per unit area of the crystal. The following formula determines it [25]:

$$\delta = \frac{1}{t^2} \tag{2}$$

The optical system under current investigation consists of SAHQ-x film of uniform thickness deposited onto optical flat amorphous quartz substrate. A double beam spectrophotometer (JASCO model V-570-UV–vis.–NIR) gives the spectral data of the transmittance, $\boldsymbol{T}$ (λ), and the reflectance, $\boldsymbol{R}$ (λ), at nearly normal incidence of the light in the spectral wavelength range 200–2500 nm. The experimental values of the total measured transmittance, $T_{expt.}$, and reflectance, $R_{expt.}$, after introducing corrections resulting from the absorption and reflection of the substrate have been calculated as in Ref. [26]. Murmann exact equations [27] give the theoretical values of the transmittance, $T_{theo.}$ and the reflectance, $R_{theo.}$. The computational work [28] uses the iterative technique to minimize the values of $[T_{theo.} - T_{expt.}]^2$ and $[R_{theo.} - R_{expt.}]^2$ for a fixed value of film thickness. Substituting the obtained absolute values of T and R in the following equations, we get the refractive index, the extinction coefficient and the absorption coefficient:

$$n = \left(\frac{1+R}{1-R}\right) + \sqrt{\frac{4R}{(1-R)^2} - k^2} \tag{3}$$

$$\alpha = \frac{1}{d}\left[\ln\left(\frac{(1-R)^2}{2T}\right) + \sqrt{\left(\frac{(1-R)^4}{4T^2} + R^2\right)}\right] \tag{4}$$

$$k = \frac{\alpha\lambda}{4\pi} \tag{5}$$

The experimental errors are taken into consideration as 1% for T (λ) and R (λ) and $\pm$ 3–5% for film thickness measurements.

3. Results and discussion

3.1. Structural analysis

Fig. 1 shows the XRD patterns for **SAHQ-x** ligands in powder form. The pattern for each ligand shows polycrystalline structure. We used CRYSFIRE system for automatic powder indexing [29] to calculate the indicated Miller indices (hkl) on each diffraction peak. Fig. 2 shows the XRD patterns for SAHQ-x ligands thin films with thickness 223 nm. The substitution group variation influences the XRD patterns. The XRD patterns of Cl and NO_2 substituent show some diffraction peaks with a halo in the background. The broad halo in the background is either due to the amorphous glass substrate or possibly due to some amorphous phase present in the thin film. The XRD pattern of SAHQ-NO_2 shows four diffraction peaks at (2θ) of 5.5, 6.2, 9.7 and 29.25° and XRD pattern of SAHQ-Cl shows one diffraction peak at (2θ) of 7.12°. This indicates that the degree of crystallinity of SAHQ-NO_2 is better than that one of SAHQ-Cl .The determined crystallite size and dislocation density are 70.7 nm and 2×10^{-4} nm^{-2}, respectively for SAHQ-NO_2 and they are 64 nm and 2×10^{-4} nm^{-2}, respectively for SAHQ-Cl. The XRD of SAHQ-CH_3 shows an amorphous structure.

3.2. Spectral behavior of T (λ) and R (λ)

The spectral behavior of the transmittance, T (λ), and the reflectance, R (λ), at nearly normal incidence of light for the as deposited SAHQ-x; $x = NO_2$ or CH_3 or Cl ligands thin films of thickness 223 nm is presented in Fig. 3. This spectrum shows a transmission edge whose wavelength range depends on the substitution group. There are two regions in the spectra: region (I) is in the wavelength range 200–834 nm, where the total sum of T (λ) and R (λ) is less than unity (absorption region) and region (II) is for the wavelengths greater than 834 nm where T (λ) + R (λ) = 1(transparent region). In this region the film becomes transparent i.e. no absorption takes place. The results of T (λ) and R (λ) indicate that the film is homogeneous. In all cases, we do not observe new transmission peaks. Therefore, substitution group variation has no change on the transmittance properties of the films in the absorption region of the spectra.

3.3. Spectral behavior of optical functions of SAHQ-x

The spectral distribution of the refractive index, n, for SAHQ-x, $x = NO_2$ or CH_3 or Cl ligands thin films with thickness 223 nm is shown in Fig. 4. The refractive index, n, does not only depend on wavelength, λ but also on type of the substitution group. The variation of refractive index with changing substitution group is attributed to the structural changes occurred on SAHQ by substituent as shown in Fig. 2. The dispersion curve shows two bands for SAHQ-CH_3, one band and a shoulder for SAHQ-NO_2 and two
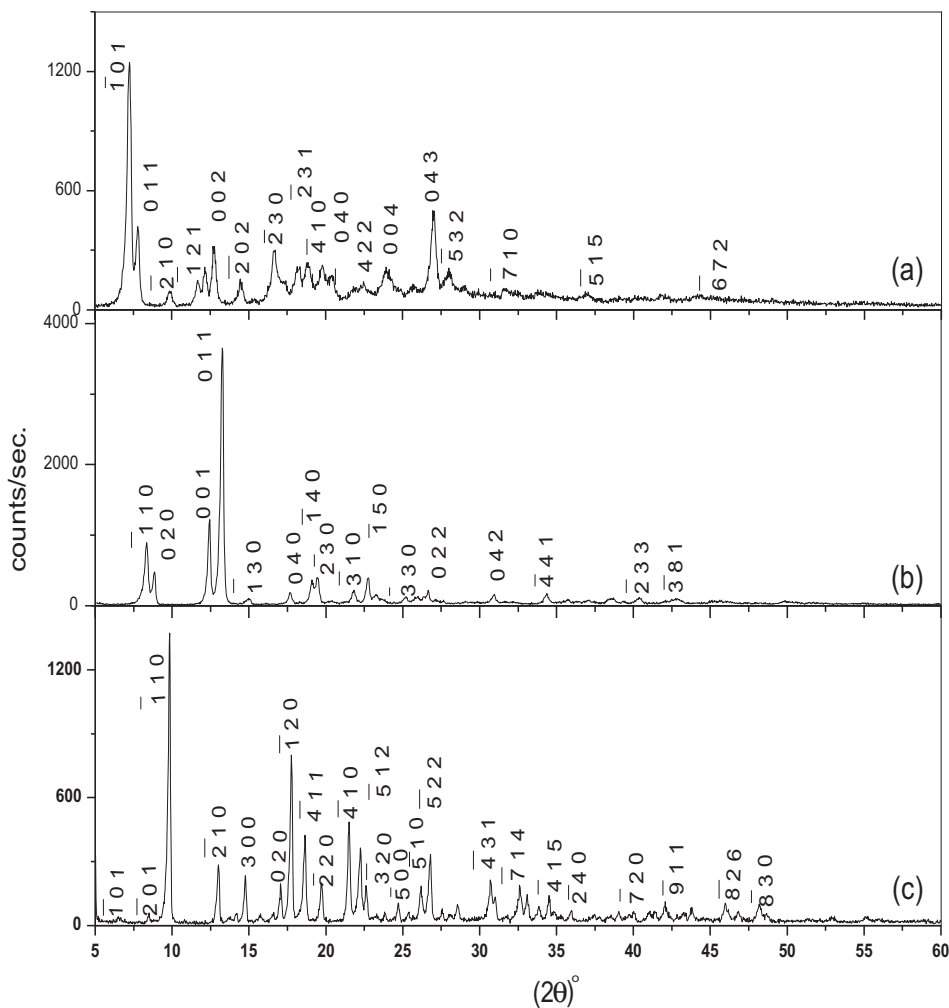
Fig. 1. XRD patterns for the powder of SAHQ-x ligands; (a) x = NO$_2$, (b) x = CH$_3$ and (c) x = Cl.

bands and a shoulder for SAHQ-Cl. These bands are located in the ultraviolet and visible regions of spectra and are attributed to π–π* transitions. Therefore, multi-oscillator model can explain such bands. At wavelengths longer than 854 nm, the spectral behavior of n shows normal dispersion which can be explained by the single oscillator model. In this wavelength range, we can deduce the dielectric constants and oscillator parameters at high frequencies.
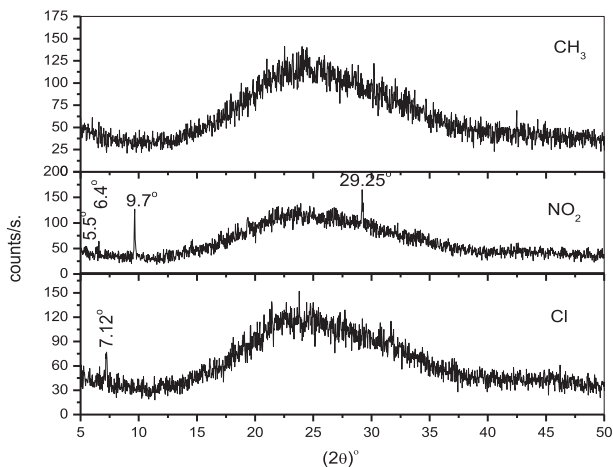

Fig. 2. XRD patterns for the thin films of SAHQ-x ligands; (a) x = NO$_2$, (b) x = CH$_3$ and (c) x = Cl.
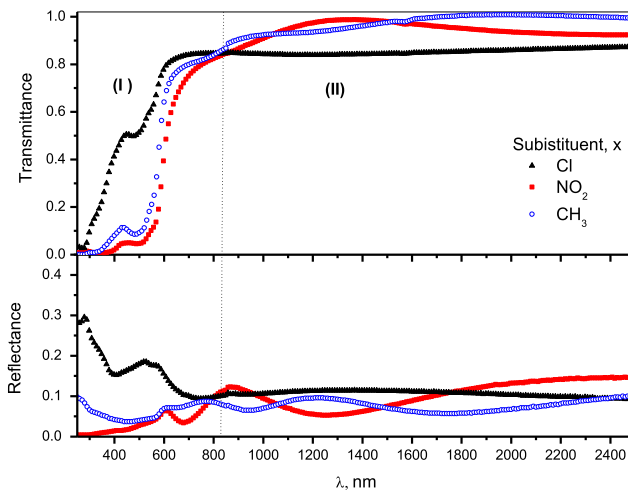

Fig. 3. Spectral behavior of the transmittance, $T(\lambda)$, and the reflectance, $R(\lambda)$, for the as deposited SAHQ-x ligands thin films.
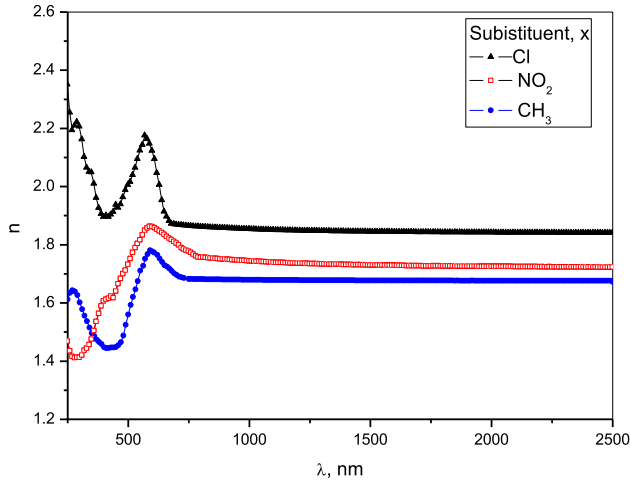
Fig. 4. Spectral behavior of refractive index, n, for the as deposited SAHQ-x ligands thin films.

The dispersion theory [30] relates the refractive index n to the dispersion parameters by:

$$\frac{1}{n^2 - 1} = \frac{E_o}{E_d} - \frac{1}{E_o E_d}(h\nu)^2 \qquad (6)$$

A plot of $(n^2 - 1)^{-1}$ versus $(h\nu)^2$ for films in the as deposited condition is illustrated in Fig. 5. The oscillator energy, E_o, and the dispersion energy, E_d, are directly determined from the slope $(E_o E_d)^{-1}$ of the linear portion of the curve and its intercept with the ordinate axis (E_o/E_d). The physical meaning of E_o and E_d is mentioned elsewhere [18]. Table 1 lists the calculated values of the dispersion parameters for SAHQ-x ligands thin films. The oscillator energy E_o and the dispersion energy E_d have been reported to be related to the bond length, L, via $E_o \propto L^{-s}$ [31] and E_d depends on L^s [32] with s in the range $2 < s < 3$ [31]. The dependence of E_o and E_d on the substituent indicates that substitution group variation influences the bond length of SAHQ compound.

Dielectric function relates the electron transitions between bands of a solid to its structure. Therefore, we can obtain valuable information about the ban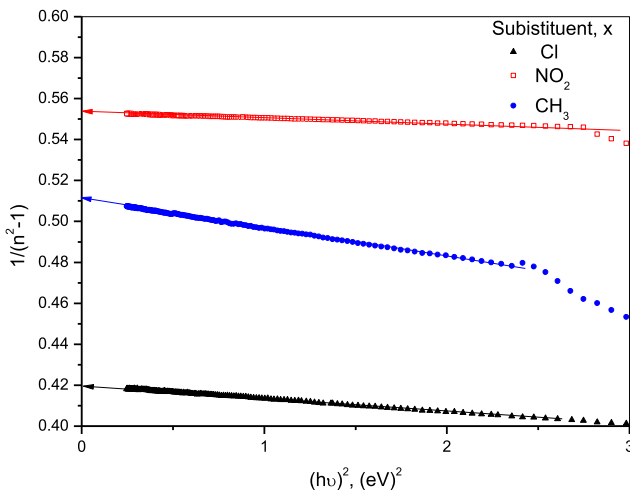d structure of a solid from dielectric spectrum. The real, ε_1, and the imaginary, ε_2, parts of the complex dielectric constant, ε^*, are respectively given by Ref. [33]:

$$\varepsilon_1 = n^2 - k^2 = \varepsilon_L - \left(\frac{e^2}{4\pi^2 c^2 \varepsilon_o}\right)\left(\frac{N}{m^*}\right)\lambda^2, \qquad (7)$$

$$\varepsilon_2 = 2nk = \frac{\varepsilon_\infty \omega_p^2}{8\pi^2 c^3 \tau}\lambda^3, \quad \omega_p = \left(\frac{e^2 N}{\varepsilon_o \varepsilon_L m^*}\right)^{1/2} \qquad (8)$$

where ω_p is the plasma frequency, ε_L is the lattice dielectric constant, ε_o is the permittivity of free space, N/m^* is the ratio of free carrier concentration to its effective mass and τ is the optical relaxation time. The spectral distribution of $(n^2 - k^2)$ versus λ^2 is depicted in Fig. 6. Substitution group variation influences the value of $(n^2 - k^2)$. The values of the lattice dielectric constant (ε_L) for SAHQ-x ligands thin films are determined by extrapolating the curves to intercept the ordinate axis. The values of N/m* are deduced from the slope of the linear portion of the curves. The values of ε_L and N/m* are listed in Table 1. We can see from Table 1 that the value of ε_L is greater than the value of ε_∞ and this is ascribed to free carrier absorption.

Fig. 7 illustrates the real part of the dielectric constant versus photon energy and substitution group variation for SAHQ-x ligands thin films. The real dielectric constant shows different response to the increase of photon energy that depends on the substitution group. Absorption peaks for ε_1 are observed at 2.14, 3.48 and 4.04eV for the as deposited SAHQ-Cl film and at 2.01 and 3eV for SAHQ-NO$_2$ ligand. As for SAHQ-CH$_3$ ligand, it shows absorption peaks at 2.09 and 4.8eV.

Fig. 8 shows the dependence of the imaginary part of the dielectric constant on photon energy and substituent variation for SAHQ-x ligands thin films. ε_2 increases with the increase of photon energy. The onset absorption edge depends on the substitution group for the SAHQ. The optical energy gaps are determined from
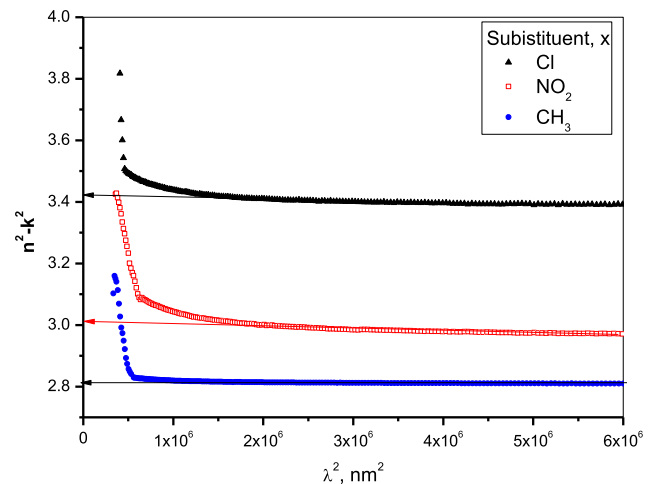
Table 1
Effect of substitution group variation on the dispersion and dielectric parameters of SAHQ-x ligands.

Substitution, x	E_o (eV)	E_d (eV)	ε_∞	ε_L	N/m*x10^{53} (kg^{-1} m^{-3})
Cl	8.44	20.15	3.39	3.42	23
NO$_2$	6.06	11.86	2.96	3	37
CH$_3$	14.6	26.42	2.8	2.81	9

Fig. 5. Dependence of $(n^2 - 1)^{-1}$ on $(h\nu)^2$ for the as deposited SAHQ-x ligands thin films.

Fig. 6. Dependence of $(n^2 - k^2)$ on λ^2 for the as deposited SAHQ-x ligands thin films.
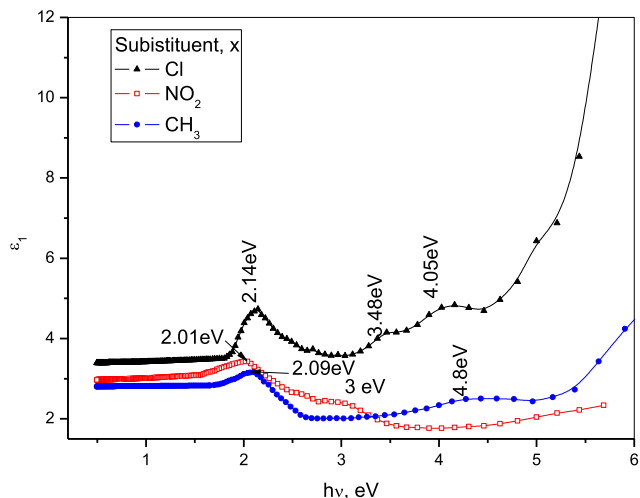
Fig. 7. Spectral behavior of ε_1 for the as deposited SAHQ-x ligands thin films.
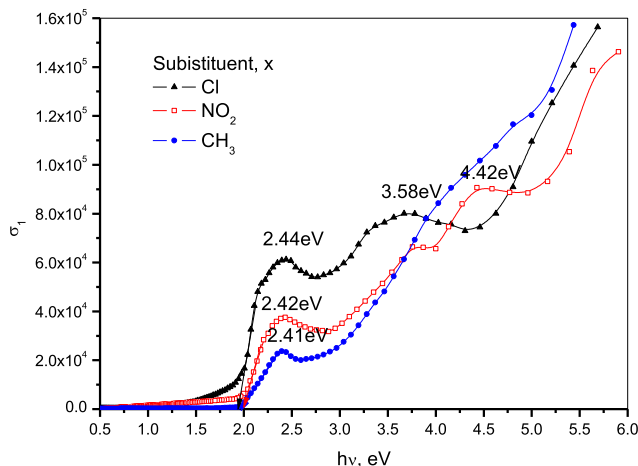

Fig. 9. Spectral behavior of the real part of electrical conductivity σ_1 for the as deposited SAHQ-x ligands thin films.

the intersection of the onset absorption edge with the abscissa of Fig. 8. The determined optical energy gaps are 1.89, 2 and 2 eV for SAHQ-x, x = NO$_2$ or CH$_3$ or Cl ligands, respectively.

The real, σ_1, and imaginary, σ_2, part of the optical conductivity can be used to detect any further allowed interband optical transitions. The following relation expresses the complex optical conductivity σ^* in terms of σ_1 and σ_2 [34] as:

$$\sigma^*(\omega) = \sigma_1(\omega) + i\sigma_2(\omega) \tag{9}$$

where

$$\sigma_1(\omega) = \omega\varepsilon_0\varepsilon_2 \tag{9a}$$

$$\sigma_2(\omega) = \omega\varepsilon_0\varepsilon_1 \tag{9b}$$

Fig. 9 demonstrates the spectral behavior of the real part of the optical conductivity and its variation with substituent. σ_1 increases with the increase of the photon energy. σ_1 is near zero for photon energies near 1.5 eV. The behavior of σ_1 with photon energy depends on the substituent. The onset absorption edge depends on the type of substitution group. The optical energy gap of (SAHQ-x), x = NO$_2$ or CH$_3$ or Cl ligands are 1.89, 2 and 2 eV, respectively.

Fig. 10 illustrates the spectral behavior of the imaginary part of the optical conductivity, σ_2. The value of σ_2 is greater than the value of σ_1 for the same substitution group. σ_2 is near zero for photon energies less than 1.5 eV σ_2 increases with the increase of the photon energy. The effect of Cl as a substituent on σ_2 is higher than the effect of NO$_2$ and CH$_3$ substituent, for all substitution groups we observe a peak of energy at 2.1 eV.

The energy loss functions provide a complete description of the response of the material to fast electrons traveling either through its bulk or on its surface. The surface energy loss, SEL and the volume energy loss, VEL, relate to the real and imaginary parts of the dielectric constant by the following relationships [35]:

$$SEL = \frac{\varepsilon_2}{(\varepsilon_1 + 1)^2 + \varepsilon_2^2} \tag{10}$$

$$VEL = \frac{\varepsilon_2}{(\varepsilon_1^2 + \varepsilon_2^2)} \tag{11}$$

Figs. 11 and 12 show the surface energy loss, SEL, and the volume energy loss, VEL, as a function of the incident photon energy. Both functions have the same behavior and the energy lost by electrons traveling through the material is greater than the energy lost by
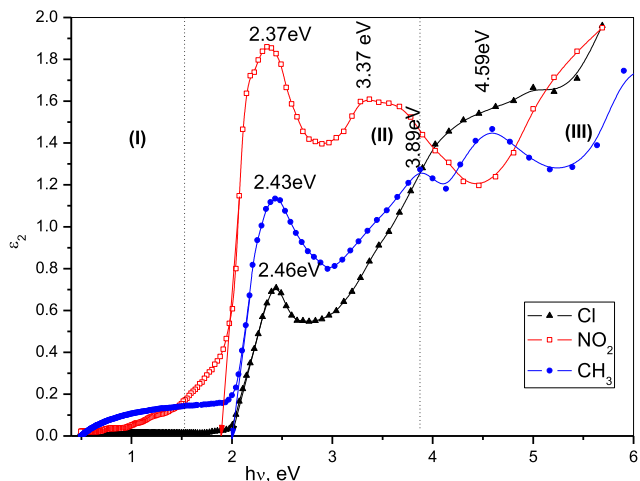

Fig. 8. Spectral behavior of ε_2 for the as deposited SAHQ-x ligands thin films.
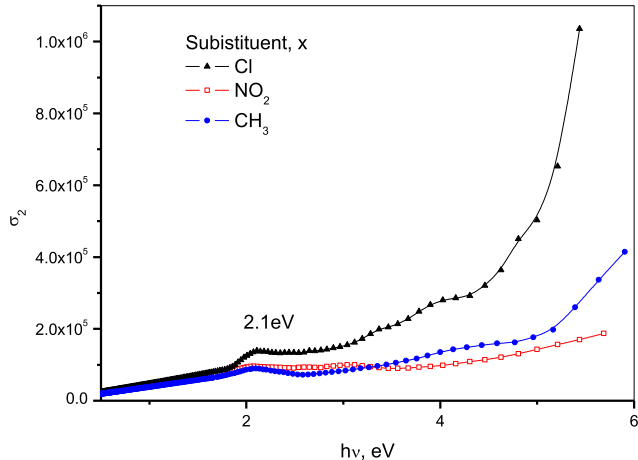

Fig. 10. Spectral behavior of the imaginary part of electrical conductivity σ_2 for the as deposited SAHQ-x ligands thin films.
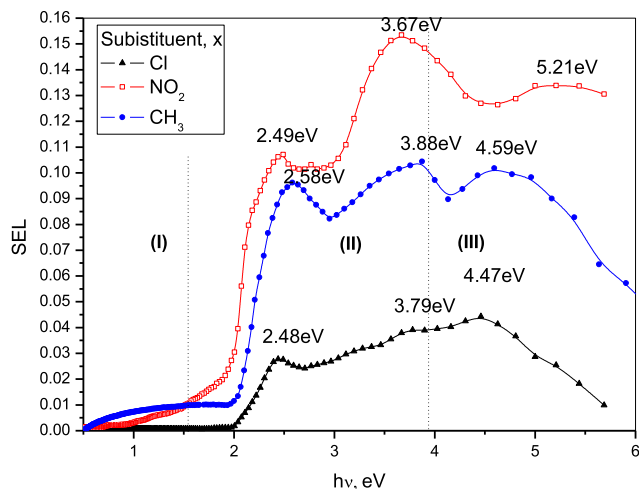
Fig. 11. Spectral behavior of the surface energy loss for the as deposited SAHQ-x ligands thin films.

electrons traveling in its surface. Photon energy influences both VEL and SEL and they show different response depending on the substitution group. The spectra of SEL and VEL functions can be divided into three energy regions depending on the frequency of the incident light. In the low energy region (hν < 2eV); a slow increase of energy loss functions with increasing photon energy is observed, such an increase depends on the type of the substitution group. In region II (2 < hν < 4 eV); an onset absorption edge is observed and its range depends on the type of substituent. A larger energy loss peak follows in energy range of 3.67–3.88 eV depending on the type of the substituent. This peak corresponds to the energy of SAHQ plasma [36]. In region III (4 < hν < 5.8 eV) the energy loss function decreases with increasing of photon energy.

We can calculate the mobility, μ, of charge carriers by the following relationship:

$$\mu = \frac{e\tau}{m} \qquad (12)$$

τ is the relaxation time, τ values are determined by using the relationship ($\omega_p \tau = 1$) for ω_p values obtained from the maximum peak values of VEL (Fig. 12). Table 2 lists values of μ, τ and ω_p for
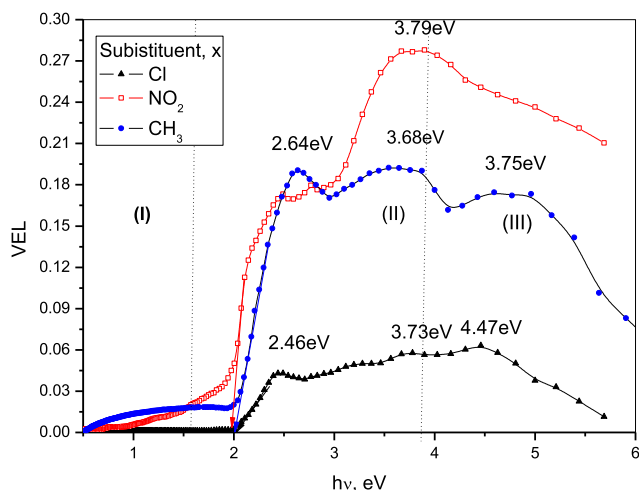

Fig. 12. Spectral behavior of the volume energy loss for the as deposited SAHQ-x ligands thin films.

Table 2
Effect of substitution group variation on the plasma frequency, ω_p, relaxation time, τ, and mobility of charge carriers of SAHQ-x ligands.

Substitution, x	$\omega_p \times 10^{15}$ (Hz)	$\tau \times 10^{16}$ (s)	$\mu \times 10^{-5}$ (m^{2}V^{-1}s^{-1})
Cl	5.67	1.76	3.09
NO$_2$	5.76	1.73	3.05
CH$_3$	5.59	1.78	3.14

SAHQ-x, x = NO$_2$ or CH$_3$ or Cl ligands. Substituent variation has no influence on μ, τ and ω_p of charge carriers in SAHQ-x ligands.

4. Conclusions

The main conclusions of the current investigation can be summarized as; -5-sulfono-7-(4-x phenyl azo)-8-hydroxy quinoline (SAHQ)-x, x = NO$_2$ or CH$_3$ or Cl ligands have polycrystalline structure in the as synthesized condition, SAHQ-NO$_2$ and SAHQ-Cl become nano-crystalline structure upon thermal deposition to be thin films. Thermally evaporated thin films of SAHQ-CH$_3$ have amorphous structure. Substitution group variation has no change on the transmittance properties of the films in the absorption region of the spectra. Substituent variation influences the refractive index, the oscillator energy, E_o, the dispersion energy, E_d, and the bond length of SAHQ compound. We determined the optical energy gaps as 1.89, 2 and 2eV for SAHQ-x, x = NO$_2$ or CH$_3$ or Cl ligands, respectively. Substitution group variation has no influence on the mobility, relaxation time and plasma frequency of charge carriers in SAHQ-x ligands.

References

[1] A.D. Dorneick, R.H. French, H. Müllejans, S. Loughin, M. Ruhle, J. Microsc. 191 (1998) 286–296.
[2] G.L. Tan, M.F. Lemon, R.H. French, J. Am. Ceramic Soc. 86 (2003) 1885–1892.
[3] W. Werdecker, F. Aldinger, IEEE Trans. Components Hybrids Manufac. Technol. 7 (1984) 399–404.
[4] C. Festenberg, Z. Physik 227 (1969) 453–481.
[5] L. Xiao, Y. Liu, Q. Xiu, L. Zhang, Tetrahedron 66 (2010) 2835–2841.
[6] B. Adhikari, S. Majumdar, Prog. Poly. Sci. 29 (2004) 699–766.
[7] C.Y. Kwong, A.B. Djurisic, W.C.H. Choy, M.H. Xie, Mater. Sci. Eng. B 116 (2005) 75–81.
[8] J. Xie, Z. Ning, H. Tian, Tetrahedron Lett. 46 (2005) 8559–8562.
[9] W.A.E. Omar, H. Haverinen, O.E.O. Hormi, Tetrahedron 65 (2009) 9707–9712.
[10] S.K. Saha, Y.K. Su, F.S. Juang, IEEE J. Quantum Electron. 37 (2001) 807–812.
[11] Y. Qiu, Y. Shao, D. Zhang, X. Hong, Jpn. J. Appl. Phys. 39 (2000) 1151–1153.
[12] X.C. Li, Y. Jia, S. Li, Eur. Polym. J. 27 (1991) 1345–1351.
[13] M. Kurihara, A. Hirooka, S. Kume, M. Sugimoto, H. Nishihara, J. Am. Chem. Soc. 124 (2002) 8800–8801.
[14] K. Yamaguchi, S. Kume, K. Namiki, M. Murata, N. Tamia, H. Nishihara, Inorg. Chem. 44 (2005) 9056–9067.
[15] R.H. El Halabieh, O. Mermut, C.J. Barrett, Pure Appl. Chem. 76 (7–8) (2004) 1445–1465.
[16] H.M. Zeyada, M.M. EL-Nahass, I.S. Elashmawi, A.A. Habashi, J. Non-crystalline Solids 358 (2012) 625–636.
[17] H.M. Zeyada, M.M. EL-Nahass, S.A. Samak, J. Non-crystalline Solids 358 (2012) 915–920.
[18] H.M. Zeyada, M.M. EL-Nahass, M.M. EL-Shabaan, J. Mater. Sci. 47 (2012) 493–501.
[19] Ka. E. Lee, M. Wang, Eui. J. Kim, S.H. Hahn, Curr. Appl. Phys. 9 (2009) 683–687.
[20] P.G. Collins, K. Bradley, M. Ishigami, A. Zettle, Science 287 (1982) 4205–4213.
[21] N.A. El-Ghamaz, M.A. Diab, A.Z. El-Sonbati, O.L. Salem, Spectrochim. Acta Part A 83 (2011) 61–66.
[22] M.S. Masoud, E.A. Khalil, A.M. Hindawy, A.E. Ali, E.F. Mohammed, Spectrochim. Acta A 60 (2004) 2807–2817.
[23] M.S. Sujamol, C.J. Athira, Y. Sindhue, K. Mohanan, Spectrochim. Acta A 75 (2010) 106–112.
[24] C. Hammond, The Basics of Crystallography and Diffraction, third ed., Oxford University Press, 2009.
[25] S. Velumani, X. Mathew, P.J. Sebastian, Solar Energy Mater. Solar Cells 76 (2003) 359–368.
[26] M.M. El-Nahass, J. Mater. Sci. 27 (1992) 6597–6604.
[27] O.S. Heavens, in: G. Hass, R. Thus (Eds.), Physics of Thin Films, Academic Press, New York, 1964, p. 193.
[28] M.M. El-Nahass, H.M. Zeyada, M.S. Aziz, N.A. El-Ghamaz, Opt. Mater. 27 (2004) 491–498.

[29] R. Shirley, The CRYSFIRE 2002 System for Automatic Powder Indexing: User's Manual, The Lattice Press, 41 Guildford Park Avenue, Guildford, Surrey GU2 7NL, England, 2002.
[30] S.H. Wemple, M. DiDomenico, Phys. Rev. B 3 (1971) 1338–1351.
[31] H. Chen, W.Z. Shen, Eur. Phys. J. B 43 (2005) 503–507.
[32] J.M. González-Leal, J.A. Ángel, E. Márquez, R. jiménez-Garay, J. Phys. Chem. Solids 68 (2007) 987–992.
[33] P.O. Edward, Hand Book of Optical Constants of Solids, Academic Press, New York, 1985.
[34] F. Yakuphanoglu, M. Sekerci, O.F. Oztuk, Opt. Commun. 239 (2004) 275–280.
[35] M.M. El- Nahass, Z. El-Gohary, H.S. Soliman, Opt. Laser Technol. 35 (2003) 523–531.
[36] Y. Du, B. Chang, X. Fu, X. Wang, M. Wang, Optik 123 (2012) 2208–2212.